IRAQI JOURNAL OF MATERIALS
Volume (4) Issue (1) January-March 2025, pp. 23-30

Synthesis of Titanium Nitride Nanostructures by Microwave-Induced Reaction of Titanium(IV) Chloride with Ammonia

Jason M. Fraser, Rosaline S. McCormack

Department of Chemistry, Faculty of Science, University of Brantford, Brantford, UK

Abstract
In this work, a chemical reaction of titanium chloride with ammonia was initiated and induced by microwaves in order to synthesize titanium nitride nanopowders. Different powers of microwaves as well as induction times were used to study their effects on the structural characteristics of the synthesized nanopowders. The effect of microwave power was observed in decreasing the particles size within the nanopowder while the effect of induction time was observed in allowing more crystal planes to grow within the structure of the synthesized nanopowders.

Keywords: Titanium nitride; Microwaves; Structural characteristics; Nanopowders
Received: 15 August 2024; **Revised:** 11 October 2024; **Accepted:** 18 October; **Published:** 1 January 2025

1. Introduction

Nanopowders are ultrafine particles with dimensions in the nanometer range (1-100 nm), characterized by a high surface area-to-volume ratio and unique physicochemical properties. These materials have garnered significant attention in various fields, including catalysis, energy storage, and advanced coatings, due to their exceptional reactivity, mechanical strength, and tunable properties. Among these, titanium nitride (TiN) nanopowders stand out for their remarkable combination of electrical conductivity, thermal stability, and chemical inertness [1-3].

Titanium nitride (TiN) is a ceramic material known for its exceptional hardness, wear resistance, and high melting point. It is typically golden-yellow in color and exhibits metallic conductivity [4,5]. TiN's properties make it highly suitable for applications in cutting tools, decorative coatings, and electronic components [6]. When synthesized in nanopowder form, TiN demonstrates enhanced surface reactivity and optical properties, making it an excellent candidate for advanced technological applications [7,8].

Electromagnetic radiation plays a crucial role in accelerating chemical reactions for synthesizing nanomaterials without requiring sophisticated setups [9,10]. By providing energy to reaction systems, electromagnetic waves (e.g., ultraviolet (UV), visible light, microwave, or infrared (IR)) can induce or enhance chemical transformations, enabling precise control over reaction rates and product morphology. For instance, UV and visible light can excite electrons in reactants or catalysts, generating reactive species like radicals or electron-hole pairs that drive reactions more efficiently. This approach is commonly utilized in photochemical synthesis, where light-sensitive precursors produce nanomaterials like metal oxides, quantum dots, or photocatalysts with high precision [11-13]. Microwave radiation offers rapid, uniform heating at the molecular level, significantly reducing reaction times compared to conventional methods [14]. It enhances reaction kinetics by directly interacting with polar molecules and solvents, promoting the formation of nanostructures with controlled size and shape [15,16]. Moreover, microwaves enable solvent-free or low-solvent reactions, making the process environmentally friendly [17,18]. Infrared radiation aids in heating reaction systems selectively, minimizing energy wastage and improving reaction efficiency [19,20]. The simplicity of setups involving electromagnetic radiation makes this approach cost-effective and accessible, especially in resource-limited settings [21,22]. Overall, electromagnetic radiation provides a sustainable, energy-efficient

pathway for producing high-quality nanomaterials, revolutionizing fields like catalysis, energy storage, and biomedical applications [23,24].

Microwave-assisted chemical synthesis is an innovative method for producing nanopowders, including TiN [25]. This technique utilizes microwave radiation to provide rapid, uniform heating at the molecular level, significantly reducing reaction times compared to conventional methods [26]. For TiN nanopowders, precursors such as titanium salts (e.g., titanium chloride) and nitrogen sources (e.g., ammonia or urea) are mixed in a suitable solvent [27]. When exposed to microwave energy, the reaction proceeds efficiently, forming TiN nanoparticles [28]. This method offers several advantages, including energy efficiency, precise control over reaction parameters, and the ability to achieve high purity and uniform particle size distribution [29].

TiN nanopowders are widely used in protective coatings for cutting tools, medical implants, and decorative applications [30]. Their high hardness and wear resistance improve the durability and performance of coated surfaces [31]. Due to their excellent electrical conductivity and thermal stability, TiN nanopowders are used in microelectronics as electrodes, interconnects, and diffusion barriers in integrated circuits [32]. TiN nanopowders serve as electrode materials in supercapacitors and lithium-ion batteries [33]. Their high conductivity and stability enhance charge storage and cycling performance. TiN nanoparticles exhibit plasmonic properties similar to gold, making them suitable for applications in photonic devices, sensors, and surface-enhanced Raman spectroscopy [34]. TiN's high surface area and chemical stability make it an effective catalyst or catalyst support in chemical reactions, including hydrogen production and environmental remediation [35]. TiN nanopowders are used in medical implants and devices due to their biocompatibility and resistance to corrosion, reducing wear and extending the lifespan of implants [36].

2. Experimental Part

A 100 mL of titanium(VI) chloride ($TiCl_4$) was placed in a glass vessel of 8cm in diameter and an aqueous solution of ammonia (NH_3) was dropped slowly using a micropipette to avoid the sudden initiation of the chemical reaction. The mixture was left for 30 s then the vessel was transferred to a microwave chamber. The microwave shown in Fig. (1) is operated at frequency of 2.45 GHz and the heating power can be adjusted from 1.6 to 9.6 kW to reach 1000 °C during 45 s.

Fig. (1) Microwave furnace system used for inducing the chemical reaction in this work

The chemical reaction to induce is the following:

$$32\ NH_{3\ (aq)} + 6\ TiCl_{4\ (l)} \rightarrow N_{2\ (g)} + 24\ NH_4Cl_{\ (aq)} + 6\ TiN_{\ (s)}$$

The reaction between ammonia (NH_3) and titanium tetrachloride ($TiCl_4$) produces nitrogen gas (N_2), ammonium chloride (NH_4Cl), and titanium nitride (TiN). In aqueous solution, ammonia reacts with $TiCl_4$ to reduce titanium ions, forming solid titanium nitride and releasing nitrogen gas [37]. Ammonium chloride, a byproduct, remains in the aqueous phase. The balanced equation shows that for every 32 moles of ammonia, 6 moles of titanium tetrachloride are consumed, producing 6 moles of titanium

nitride, 24 moles of ammonium chloride, and 1 mole of nitrogen gas. This reaction is an example of a reduction and precipitation process in a controlled environment.
This reaction is slow and producing nitrogen gas, which is removed from the chemical reaction volume to avoid the overdosed nitriding of titanium released from the chloride precursor [38]. However, this extraction should compensate the required amount to produce titanium nitride (TiN) with the aimed specifications.
As soon as the golden color is seen within the produced solid product (Fig. 2), the reaction vessel should be taken out the microwave furnace system, closed well, and left in the room environment for 2 hours to allow the formation step to complete.
To remove NH_4Cl aqueous solution from the product of a chemical reaction, several strategies can be used depending on the properties of the product and reaction conditions. Since NH_4Cl is soluble in water, the water can be evaporated leaving behind NH_4Cl as a solid (if it is part of a precipitate) or removing it entirely if it remains dissolved. If NH_4Cl crystallizes upon cooling or partial evaporation, the reaction mixture is cooled to promote crystallization [39]. Vacuum or gravity filtration can be used to separate the solid NH_4Cl from the liquid product. Alternatively, the mixture can be centrifuged if fine particulates are present. This method may lead to an increase in the particle size of titanium nitride (TiN) nanopowder due to the thermal accumulation effects [40].
Using a solvent in which the product is soluble but NH_4Cl is not (e.g., organic solvents like ethyl acetate or chloroform if the product is organic). The product is extracted into the organic layer, leaving NH_4Cl in the aqueous layer [41]. This method is not preferred as an additional step to separated the titanium nitride (TiN) from the organic layer is highly required.

Fig. (2) TiN nanopowder collected from this work

The NH_4Cl sublimes at approximately 338°C, so, the mixture can be heated in a controlled environment to sublime NH_4Cl. The titanium nitride (TiN) should ensured to be stable at this temperature. Finally, the sublimed NH_4Cl is collected separately. This method may include unintentional heating to the titanium nitride (TiN) nanopowder, which may lead again to increase the particle size or change the structural characteristics [42].
As the NH_4Cl is soluble in water and titanium nitride (TiN) product is insoluble, then the product can be separated by filtration, leaving NH_4Cl in the aqueous solution. The solid product is washed thoroughly with water to remove residual NH_4Cl [43]. This method was used in this work. Heating during filtration can enhance the separation of NH_4Cl and TiN by increasing the solubility of NH_4Cl in water, ensuring it remains dissolved. Simultaneously, TiN, being insoluble, can be efficiently separated as a solid residue. Proper temperature control prevents premature crystallization of NH_4Cl, optimizing filtration efficiency and minimizing contamination [44].

3. Results and Discussion

The X-ray diffraction (XRD) is highly advantageous for assessing nanopowder quality. It provides precise information on crystal structure, phase composition, and lattice parameters. XRD detects impurities, identifies phases, and evaluates crystallite size and strain through peak broadening analysis. Its non-destructive nature ensures accurate characterization without altering the nanopowder's properties. Figure (3) shows the XRD patterns of the titanium nitride (TiN) nanopowder samples synthesized at different microwave powers and different induction times. The sample synthesized at 5.6 kW power of microwaves and 60 s induction time is considered the optimum as its structural

characteristics were very similar to the typical specifications of TiN nanopowder prepared by other highly-controlled synthesis methods and techniques. It is clear that the synthesized material is polycrystalline with 9 distinct diffraction peaks assigned at 2θ values of 24.915°, 37.459°, 47.697°, 53.423°, 54.799°, 62.305°, 68.476°, 69.993°, and 74.950° corresponding to crystal planes of (101), (004), (200), (105), (211), (204), (116), (220), and (215), respectively. The average crystallite size was determined by Debye-Scherrer equation to be 26 nm.

Field-emission scanning electron microscopy (FE-SEM) offers high-resolution imaging, enabling detailed surface morphology analysis of nanopowders. Its superior magnification and minimal sample damage provide precise size distribution, shape, and agglomeration insights. FE-SEM's ability to analyze conductive and non-conductive materials with minimal preparation ensures accurate quality control for nanopowder production. Figure (4) shows the FE-SEM image of the titanium nitride (TiN) nanopowder sample synthesized at 5.6 kW power of microwaves and 60 s induction time. The morphology shows high homogeneous surface with spherical particles and uniform distribution. The minimum particle size within this sample is about 2.158 nm. No aggregation of clustering is seen, which reflects the high quality of the synthesis method that attributed to the role of microwaves in producing the nanomaterial with such high specifications.

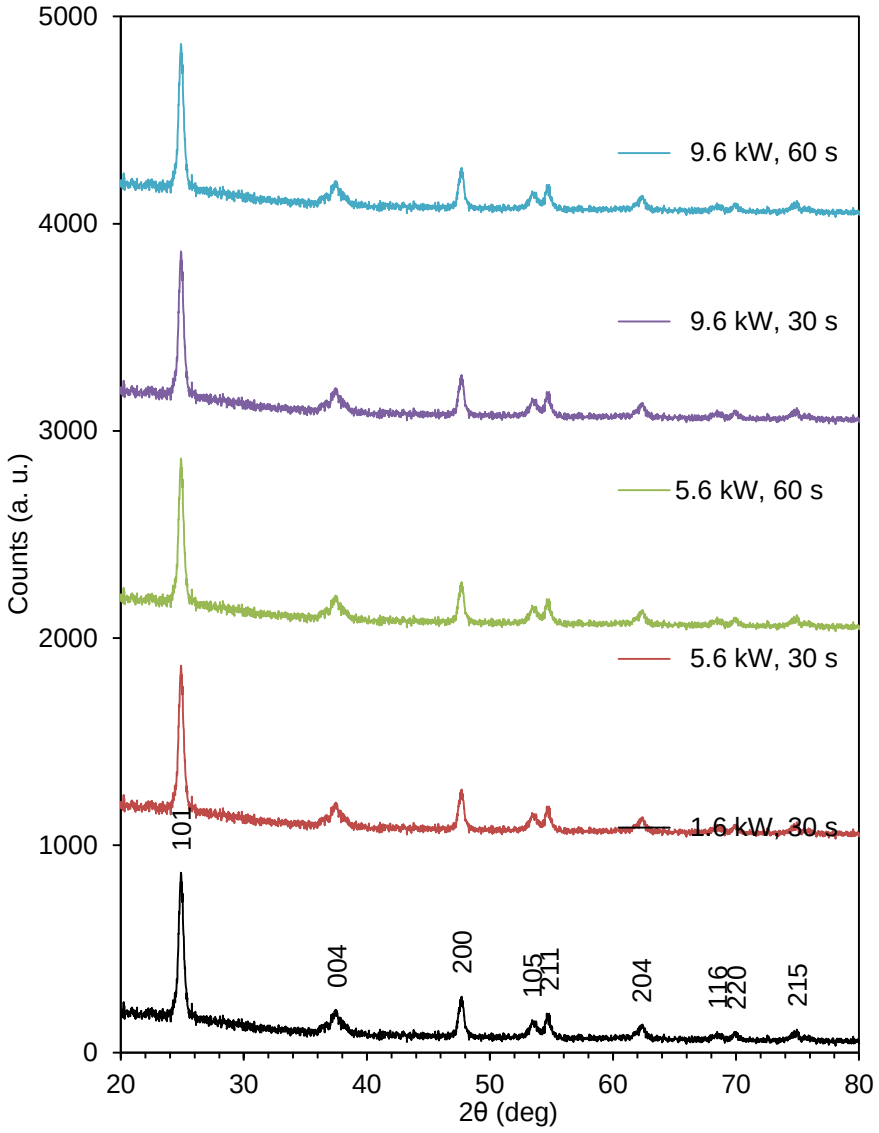

Fig. (3) XRD patterns of the TiN nanopowders synthesized in this work using different microwave powers and induction times

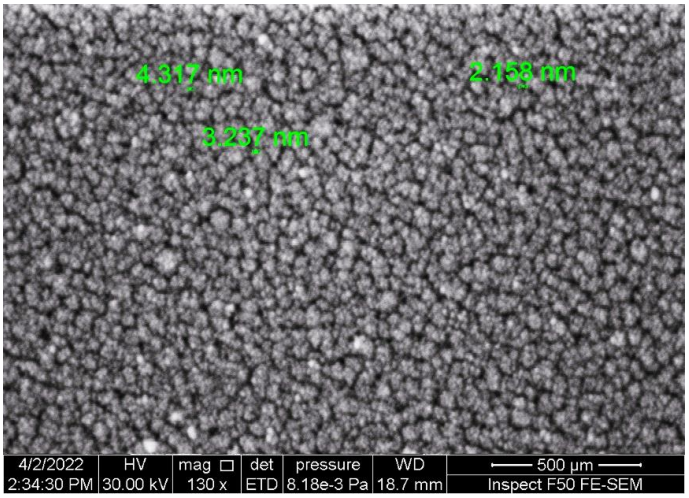

Fig. (4) FE-SEM image of the TiN nanopowder synthesized in this work using 5.6 kW microwave power and 60 s induction time

Atomic force microscopy (AFM) offers high-resolution imaging and precise topographical analysis of nanopowders. It enables measurement of particle size, shape, and surface roughness at the nanoscale. AFM provides three-dimensional visualization and quantitative data, making it ideal for assessing nanopowder uniformity, detecting defects, and ensuring consistent quality in advanced applications. Figure (5) shows the 2D and 3D AFM images of the titanium nitride (TiN) nanopowder sample synthesized at 5.6 kW power of microwaves and 60 s induction time. The nanopowder sample shows sufficiently high roughness and good surface topography with average roughness of 33.5 nm.

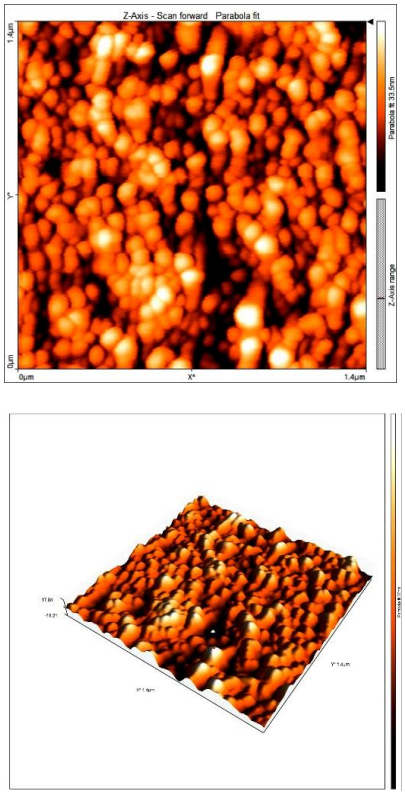

Fig. (5) 2D and 3D AFM images of TiN nanopowder synthesized in this work using 5.6 kW microwave power and 60 s induction time

Energy-dispersive x-ray spectroscopy (EDX) and color mapping provide precise elemental composition and spatial distribution of elements in nanopowders. These techniques ensure quality control by detecting impurities, verifying homogeneity, and visualizing elemental distribution at the nanoscale. They are fast, non-destructive, and crucial for optimizing nanopowder synthesis and applications. Figure (6) shows the EDX results of the titanium nitride (TiN) nanopowder sample synthesized at 5.6 kW power of microwaves and 60 s induction time. The high structural purity is clearly observed with small trace of chlorine, which inevitable product in such reaction. The color mapping of the sample shows homogeneous distribution of titanium and nitrogen particles over the sample.

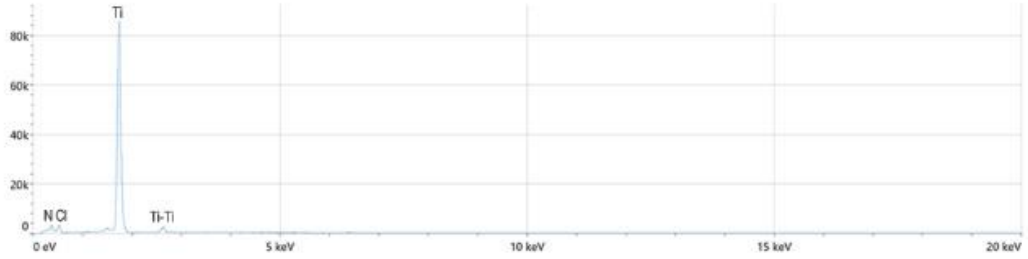

Element	Atomic %	Weight %
N	44.9	25.3
Cl	5.4	1.4
Ti	49.7	73.3

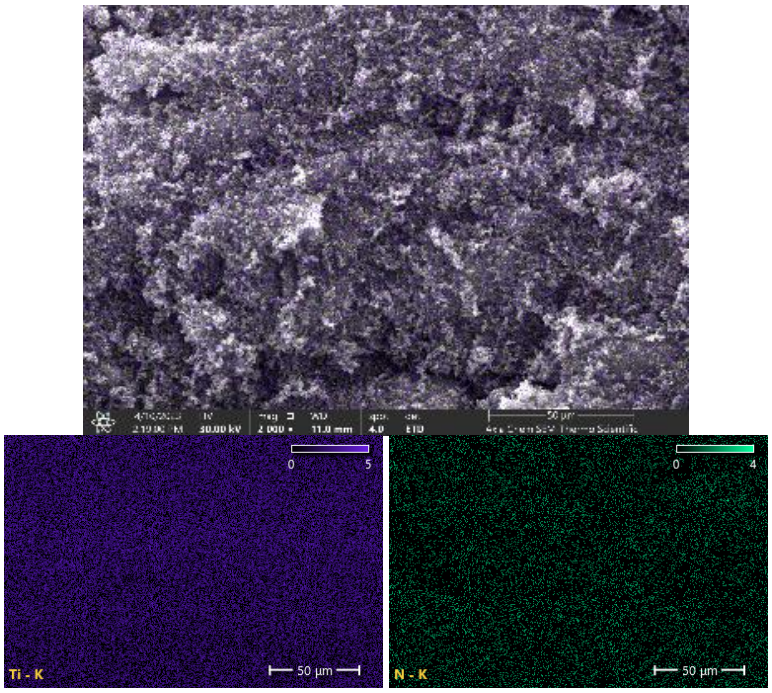

Fig. (6) EDX results of the TiN nanopowder synthesized in this work using 5.6 kW microwave power and 60 s induction time

4. Conclusions

In concluding remarks, a chemical reaction of titanium chloride with ammonia was initiated and induced by microwaves in order to synthesize titanium nitride nanopowders. Different powers of microwaves as well as induction times were used to study their effects on the structural characteristics of the synthesized nanopowders. The effect of microwave power was observed in decreasing the particles size within the nanopowder while the effect of induction time was observed in allowing more crystal planes to grow within the structure of the synthesized nanopowders.

References

[1] A.Y. Vorobyev, C. Guo, Multifunctional surfaces produced by femtosecond laser pulses. J. Appl. Phys. 117, 033103:1–5 (2015)
[2] A.Y. Vorobyev, C. Guo, Direct femtosecond laser surface nano/microstructuring and its applications. Laser Photonics Rev 7, 3 (2013)
[3] J. Bonse, S.V. Kirner, S. Höhm, N. Epperlein, D. Spaltmann, A. Rosenfeld, J. Krüger, Applications of laser-induced periodic surface structures (LIPSS), Invited Paper Proc. of SPIE Vol. 10092
[4] C. Yao, S. Xu, Y. Ye, Y. Jiang, R. Ding, W. Gao, X. Yuan, The influence of femtosecond laser repetition rates and pulse numbers on the formation of micro/nano structures on stainless steel. J. Alloys Compd. 722, 235–241 (2017)
[5] N. Yasumaru, K. Miyazaki, J. Kiuchi, Fluence dependence of femtosecond-laser-induced nanostructure formed on TiN and CrN. Appl. Phys. A 81, 933–937 (2005)
[6] O. Armbruster, A. Naghilou, M. Kitzler, W. Kautek, Spot size and pulse number dependence of femtosecond laser ablation thresholds of silicon and stainless steel. Appl. Surf. Sci. 396, 1736–1740 (2017)
[7] J. Bonse, J. Krüger, S. Höhm, A. Rosenfeld, Femtosecond laserinduced periodic surface structures. J. Laser Appl. Vol. 24, 4 (2002)
[8] B.K.K. Nayak, M.C.C. Gupta, Self-organized micro/nano structures in metal surfaces by ultrafast laser irradiation. Optics and Lasers Eng. 48, 940–949 (2010)
[9] A. Vorobyev, C. Guo, Femtosecond laser structuring of titanium implants. Appl. Surf. Sci. 253, 7272–7280 (2007)
[10] S. Hammouti, A. Pascale-Hamri, N. Faure, B. Beaugiraud, M. Guibert, C. Mauclair, S. Benayoun, S. Valette, Wear rate control of peek surfaces modified by femtosecond laser. Appl. Surf. Sci. 357, 1541–1551 (2015)
[11] J. Bonse, S.V. Kirner, R. Koter, S. Pentzien, D. Spaltmann, J. Krüger, Femtosecond laser-induced periodic surface structures on titanium nitride coatings for tribological applications. Appl. Surf. Sci. 418(Part B), 572–579 (2017)
[12] N. Epperlein, F. Menzel, K. Schwibber, R. Koter, J. Bonse, J. Sameith, J. Krüger, J. Toepel, Influence of femtosecond laser produced nanostructures on biofilm growth on steel. Appl. Surf. Sci 418, 420–424 (2017)
[13] D. Hoeche, P. Schaaf, Laser nitriding: Investigations on the model system TiN. A review. Heat Mass Transf 47(5), 519–540 (2010)
[14] P. Schaaf, T.M. Kahle, E. Carpene, Reactive laser plasma coating formation. Surf. Coat. Technol. 200, 608–611 (2005)
[15] E. Carpene, M. Shinn, P. Schaaf, Free-electron laser surface processing of titanium in nitrogen atmosphere. Appl. Surf. Sci. 247, 307–312 (2005)
[16] E. Carpene, P. Schaaf, M. Han, K. Lieb, M. Shinn, Reactive surface processing by irradiation with excimer laser, Nd:YAG laser, free electron laser and Ti: sapphire laser in nitrogen atmosphere. Appl. Surf. Sci. 186, 195–199 (2002)
[17] J. Krüger, W. Kautek, Ultrashort pulse laser interaction with dielectrics and polymers. Adv. Polym. Sci. 168, 247–290 (2004)
[18] J.M. Liu, Simple technique for measurements of pulsed Gaussianbeam spot sizes. Opt. Lett. 7(5), 196–198 (1982)
[19] V. Belaud, S. Valette, G. Stremsdoerfer, B. Beaugiraud, E. Audouard, S. Benayoun, Femtosecond laser ablation of polypropylene: a statistical approach of morphological data. Scanning 36, 209–217 (2014)
[20] D. Nečas, P. Klapetek, Gwyddion: an open-source software for SPM dataanalysis. Centr. Eur. J. Phys. 10(1), 181–188 (2012)
[21] E. McCafferty, J.P. Wightman, An X-ray photoelectron spectroscopy sputter profile study of the native air-formed oxide film on titanium. Appl. Surf. Sci. 1431, 92–100 (1999)
[22] T. Choudhury, S.O. Saied, J.L. Sullivan, A.M. Abbot, Reduction of oxides of iron, cobalt, titanium and niobium by low-energy ion bombardment. J. Phys. D Appl. Phys. 22 8, 1185 (1989)
[23] A.F. Carley, P.R. Chalker, J.C. Rivierеand, M.W. Roberts, The identification and characterisation of mixed oxidation states at oxidised titanium surfaces by analysis of X-ray photoelectron spectra. J. Chem. Soc. Faraday Trans. 1 Phys. Chem. Condens. Phases 83(2), 351–370 (1987)
[24] N.C. Saha, H.G. Tompkins, Titanium nitride oxidation chemistry: An X-ray photoelectron spectroscopy study. J. Appl. Phys. 72(7), 3072–3079 (1992)
[25] F.F.K.S.H. Esaka, K. Furuya, H. Shimada, M. Imamura, N. Matsubayashi, H. Sato, T. Kikuchi, Comparison of surface oxidation of titanium nitride and chromium nitride films studied by X-ray absorption and photoelectron spectroscopy. J. Vac. Sci. Technol. A Vac. Surf. Films 15(5), 2521–2528 (1997)
[26] P. Prieto, R.E. Kirby, X-ray photoelectron spectroscopy study of the difference between reactively evaporated and direct sputterdeposited TiN films and their oxidation properties. J. Vac. Sci. Technol. A Vac. Surf. Films 13(6), 2819–2826 (1995)
[27] X.L. Mao, W.T. Chan, M.A. Shannon, R.E. Russo, Plasma shielding during picosecond laser sampling of solid materials by ablation in He versus Ar atmosphere. J. Appl. Phys. 74, 4915–4922 (1993)
[28] R. Buividas, M. Mikutis, S. Juodkazis, Surface and bulk structuring of materials by ripples with long and short laser pulses: recent advances. Prog. Quantum Electron. 38, 119–156 (2014)
[29] J. Bonse, A. Rosenfeld, J. Krüger, On the role of surface plasmon polaritons in the formation of laser-induced periodic surface structures upon irradiation of silicon by femtosecond laser pulses. J. Appl. Phys. 106, 104910 (2009)
[30] G.A. Martsinovskii, G.D. Shandybina, D.S. Smirnov, S.V. Zabotnov, L.A. Golovan, V.Yu.. Timoshenko, P.K. Kashkarov, Ultrashort excitations of surface polaritons and waveguide modes in semiconductors. Opt. Spectrosc 105, 67–72 (2008)
[31] J. Reif, F. Costache, M. Henyk, S.V. Pandelov, Ripples revisited: non-classical morphology at the bottom of femtosecond laser ablation craters in transparent dielectrics. Appl. Surf. Sci. 197–198, 891–895. (2002)
[32] A. Borowiec, H.K. Haugen, Subwavelength ripple formation on the surfaces of compound semiconductors irradiated with femtosecond laser pulses. Appl. Phys. Lett. 82, 4462–4464 (2003)
[33] D. Dufft, A. Rosenfeld, S.K. Das, R. Grunwald, J. Bonse, Femtosecond laser-induced periodic surface structures revisited: a comparative study on ZnO. J. Appl. Phys. 105 034908 (2009). https ://doi.org/10.1063/1.30741 06
[34] J.E. Sipe, J.F. Young, J.S. Preston, H.M. van Driel, Laser-induced periodic surface structure. I. Theory. Phys. Rev. B: Condens. Matter 27, 1141–1154 (1983)
[35] J.F. Young, J.S. Preston, H.M. van Driel, J.E. Sipe, Laser-induced periodic surface structure. II. Experiments on Ge, Si, Al, and brass. Phys. Rev. B Condens. Matter 27(2), 1155–1172 (1983)
[36] J. Schille, R. Ebert, U. Loeschner, P. Regenfuss, T. Suess, H. Exner, Micro structuring with highly repetitive ultrashort laser pulses, in Proceedings of LPM 2008 (June)—The 9th international symposium on laser precision microfabrication, Quebec, Canada

[37] J. Lehr, F. de Marchi, L. Matus, J. MacLeod, F. Rosei, A.-M. Kietzig, The influence of the gas environment on morphology and chemical composition of surfaces micro-machined with a femtosecond laser. Appl. Surf. Sci. 320, 455–465 (2014)
[38] T. Smausz, T. Csizmadia, C. Tapai, J. Kopniczky, A. Oszk, M. Ehrhardt, P. Lorenz, K. Zimmer, A. Prager, B. Hopp, Study on the effect of ambient gas on nanostructure formation on metal surfaces during femtosecond laser ablation for fabrication of low reflective surfaces. Appl. Surf. Sci. 389, 1113–1119 (2016)
[39] B.K. Nayak, M.C. Gupta, K.W. Kolasinski, Formation of nanotextured conical microstructures in titanium metal surface by femtosecond laser irradiation. Appl. Phys. A Mater. Sci. Process. 90, 399–402 (2008)
[40] S. Ju, J.P. Longtin, Effects of a gas medium on ultrafast laser beam delivery and materials processing. J. Opt. Soc. Am. B Opt. Phys. 21, 1081–1088 (2004)
[41] P.G. de Gennes, Wetting: statics and dynamics. Rev. Mod. Phys. 57, 827 (1985)
[42] 43. F.M. El-Hossary, N.Z. Negm, A.M. Abd El-Rahman, M. Raaif, A. A. Abd Elmula, Properties of titanium oxynitride prepared by RF plasma, ACES 5, 1–14 (2015)
[43] P. Bizi-Bandoki, S. Benayoun, S. Valette, B. Beaugiraud, E. Audouard, Modifications of roughness and wettability properties of metals induced by femtosecond laser treatment. Appl. Surf. Sci. 257, 5213–5218 (2011)
[44] A.-M. Kietzig, S.G. Hatzikiriakos, P. Englezos, Patterned superhydrophobic metallic surfaces. Langmuir 25(8), 4821–4827 (2009)

 ISSN (print) 2958-8960 (online) 3006-6042 Printed in IRAQ